High-Speed Imaging of the First Kink Mode Instability in a Self-Field Magnetoplasmadynamic Thruster

IEPC-2013-384

Presented at the 33rd International Electric Propulsion Conference,
The George Washington University • Washington, D.C. • USA
October 6 – 10, 2013

Jonathan A. Walker[1], Samuel Langendorf[2], Mitchell Walker[3]
Georgia Institute of Technology, Atlanta, GA, 30332, USA

Kurt Polzin[4] and Adam Kimberlin[5]
Marshall Space Flight Center, Huntsville, AL, 35812, USA

One challenge to efficient high-power magnetoplasmadynamic thruster (MPDT) operation is the 'onset' regime where high-frequency voltage oscillations appear across the thruster as the discharge current is increased above a threshold value. While their physical connection remains unclear, excitation of magnetohydrodynamic kink mode instabilities have been shown to occur at discharge current levels and mass flow rates that are commensurate with the onset regime. To further investigate this connection, the formation and quasi-steady state behavior of an argon discharge in a MPDT operating in the onset regime at discharge currents of 8 to 10 kA for a pulse length of approximately 4 ms are imaged at 26,143 fps with a frame exposure time of 10 μs. A 488-nm argon line filter with a 10-nm bandwidth and a 0.9 neutral density filter were used separately to image the time evolution of the discharge plasma. Onset thruster behavior is independently verified via the observation of high frequency voltage oscillations in the 20 kHz to 80 kHz range. Frame-by-frame analysis of the light intensity flux to the camera shows power flux levels incident on the sensor on the order of 4-6 W/m2 and discharge plasma behavior that is consistent with expected radial and azimuthal asymmetries driven by helical kink mode instabilities and azimuthal discharge plasma growth. The imaging also reveals the discharge plasma radially propagates from the cathode towards the anode before quasi-steady state operation is achieved. The temporally resolved imaging of the discharge plasma is consistent with expected kink mode behavior. Additionally, a rough stability analysis of the discharge plasma column shows that for a self-field MPDT operating at certain conditions the discharge plasma can be expected to operate in the unstable Kruskal-Shafranov regime. The experimental data are supportive of a potential link between MPDT onset behavior and the excitation of the magnetohydrodynamic instabilities.

Nomenclature

I = discharge current
$\dot{m}$ = mass flow rate
P_{ar} = pressure measurement corrected for argon

[1] NSF Graduate Fellow, School of Aerospace Engineering, jwalker30@gatech.edu
[2] Graduate Research Assistant, School of Aerospace Engineering, sammuel.langendorf@gatech.edu
[3] Associate Professor, Department of Aerospace Engineering, mitchell.walker@ae.gatech.edu
[4] Propulsion Research Engineer and MSFC In-Space Electric Propulsion Lead Investigator, Propulsion Research and Technology Applications Branch, Propulsion Systems Department, kurt.a.polzin@nasa.gov
[5] Research Engineer, Propulsion Systems Department, adam.c.kimberlin@nasa.gov

P_b = base pressure measurement
P_s = pressure measurement based on N_2
q = safety factor
B_z = magnetic field component in the axial direction
B_θ = magnetic field component in the azimuthal direction
r = distance away from the center of the plasma column
L = length of discharge channel
J_o = total plasma current
a = plasma column diameter
μ_o = permeability of free space
π = mathematical constant pi

I. Introduction

ELECTRIC propulsion (EP) systems are limited in power to the levels that can be produced by a spacecraft electrical power system. At a constant thrust efficiency and input power, electric thrusters can either generate relatively higher levels of thrust or possess highly efficient propellant utilization as characterized by a high specific impulse (I_{sp})[1]. If more power is available on a spacecraft the magnetoplasmadymanic thruster (MPDT), which typically doesn't scale well for operation below power levels of 100 kW, can offer both high I_{sp} and high thrust density relative to current state-of-the-art ion and Hall thrusters. While MPDT operation at high power is conducive to both high thrust and I_{sp}, increasing the discharge current can eventually lead to unstable thruster operation that is characterized by the onset of high-frequency discharge voltage fluctuations[2-5]. This unstable operating regime is typically referred to as "onset". During onset the MPDT suffers increased power deposition to the anode, accompanied by high anode erosion rates and typically a decrease in thruster performance. A possible explanation for the existence of the onset phenomena are plasma instabilities excited during operation[4-9].

High-power MPDTs are typically tested in the lab in a pulsed, quasi-steady manner so the power requirements and facility operating pressures are within practical operational limits. The pulse lengths are several orders of magnitude longer than the timescales over which the dominant plasma processes equilibrate, enabling relatively accurate assessment of the steady-state thruster physics without requiring long-term continuous power[5-7, 10]. In the current experiment, a pulse forming network (PFN) provides simulated transmission line power at levels of approximately 1 MW and currents of 9 kA for 3-4 ms. At these high power levels, the thruster produces both high thrust density and high I_{sp} during the pulse[8]. While sufficient for equilibration of plasma processes, the 4 ms pulse duration presents challenges in terms of data collection and measurement of thruster behavior.

From the prior work of Paganucci *et al*. [7], excitation of kink mode instabilities has been observed during onset operation in a button type cathode MPDT. These measurements were achieved using radial optical measurements and Abel inversion techniques to infer on-axis plasma characteristics. As demonstrated in Park[11], the largest source of error in this measurement is the estimation of the optical path length. At power levels greater than 1 MW, the power deposition in the cathode sheath leads to significant ablation of the electrode material, potentially complicating the estimation of the optical path-length And leading to additional problems in the estimation of plasma parameters in the mixed-component magnetohydrodynamic (MHD) fluid. To reduce the cathode current density, testing at power levels on the order 1 MW or greater requires a MPDT with a larger cathode surface, as shown in work by LaPointe and Mikellides[2]. In such a thruster, the cathode runs the entire length of the discharge channel with its presence physically reducing the optical path length available for radial measurement. In these cases, direct imaging of the discharge with a line-of-sight along the thruster axis becomes favorable over radial techniques. The use of direct line-of-sight imaging along the axis provides a unique global view of the discharge plasma in a way that is not possible with radial measurement techniques. In this paper we employ this direct imaging to visually observe asymmetries in the plasma pointing to the presence of lower-order plasma kink mode instabilities when the MPDT is operating in the onset regime. To the knowledge of the authors, time-resolved imaging of the discharge plasma's global behavior during a complete single pulse at frame rates capable of capturing lower-order kink mode dynamics has not previously been performed.

The remainder of this paper details the direct imaging measurements and identification of plasma instabilities in a self-field MPDT operation and shows that these instabilities are present during onset behavior. The outline for the remainder of this paper is as follows. First, a brief description of analytical models and empirical data that predict expected MPDT plasma instabilities under the onset operating conditions is given. Then we describe the MPDT experimental apparatus and diagnostic hardware used in the present work. Experimental observations of plasma instabilities during thruster operation are presented next, including the experimental confirmation of operation in the

onset regime. Finally there is a discussion connecting the observed MPDT plasma structures to known magnetohydrodynamic (MHD) instabilities.

II. The Onset Phenomena

To date, a substantial effort has been made in understanding the physical mechanisms that cause the onset behavior. The phenomenon is thought to be connected to instabilities typically found in an MPDT [3-5, 12]. The instabilities arise from the excitation of unstable dynamic modes of MHD plasmas. Typical onset behavior is marked by increased power deposition to the thruster walls, unsteady voltage oscillations, enhanced cathode erosion, and a reduction in MPDT overall efficiency [13]. Several empirical and numerical models have sought to delineate the regime in which an MPDT might experience onset [12]. We proceed with a short review of previous work related to the onset phenomenon and connections that have been observed between onset and the appearance of MHD kink instabilities in an MPDT. It should be noted that no explanation yet exists that fully explains the onset condition and its effects within an MPDT plasma.

A. Empirical Criterion for Onset

To achieve thruster efficiencies greater than 50%, it is necessary for the self-field MPDT to operate at discharge currents greater than 9 kA[13]. However, thrusters operating in this current regime can experience the onset of kHz to MHz-level voltage oscillations and suffer from increased anode erosion[12]. One physical explanation of the onset regime depends on the depletion of charge carriers near the anode surface at higher current levels. As the current is increased, any Lorentz body force component directed inward normal to the anode will increase and serve to push charge carriers away from the anode surface[3, 4, 12]. As the number of charge carriers are depleted from the wall, the voltage across the anode sheath must increase to maintain current conduction [4, 12]. Eventually, the charge carrier depletion is so severe that large voltage oscillations in the kHz to MHz frequency ranges are observed which maintain current conduction to the wall. The large-amplitude voltage oscillations across the sheath increase local power deposition into the anode, causes significant anode material erosion [3, 4, 12]. Extensive experimental investigations have been performed in an attempt to better understand this physical mechanism thought to drive the onset phenomena. The result of these investigations has been the formulation of a critical onset limit [12],

$$\left[\frac{I^2}{\dot{m}}\right]_{crit} = 2.5\ x\ 10^{10}\frac{A^2 s}{kg} \tag{1}$$

where I is the thruster discharge current and $\dot{m}$ is the propellant mass flow rate. Onset is expected when the ratio of $I^2/\dot{m}$ is above the critical value given in Eq. (1). Although this provides an excellent empirical formulation that predicts when to expect the onset of high frequency voltage oscillations, it does not explain the appearance of other instabilities within the rest of the plasma, including what happens to the plasma during start-up and operation.

B. MHD Kink Instability

Experimental investigation with optical, electrical, and magnetic probes suggests that operational conditions that are conducive to excitation of MHD plasma instabilities also delineate the regimes of onset[5-7, 14]. In particular, the data suggest that the excitation of large-scale kink modes is related to the onset behavior [5]. The presence of instabilities produces local variations in temperature and density that further destabilize the plasma[5, 6]. In a confined, closed-loop-type plasma accelerator one of the most basic instability modes is the kink instability, the appearance of which is characterized by the Kruskal-Shafranov stability limit[5]. The most unstable of these modes is the so called m=1, n=1 mode [7]. A modified form of the traditional Kruskal-Shafranov limit applied to MPDTs, which are coaxial geometry open-type plasma accelerators, also exists[1, 5]. Experimental evidence from co-axial gun-type plasma accelerators and MPDT numerical simulation show that the large-scale behavior of this plasma instability take on the form of a helical twisted plasma filament when the Kruskal-Shafranov limit is exceeded [5, 15].

III. Experimental Apparatus

In the following section we give a brief overview of the facilities and experimental hardware used to support the testing of a self-field MPDT operating in the critical current regime. The data acquisition systems are also described in detail below.

A. Vacuum Chamber

All of the experiments are performed in the Vacuum Test Facility-2 (VTF-2) at Georgia Tech. A schematic of VTF-2 and the relative locations of the MPDT and diagnostics are given in Fig. 1. VTF-2 is a 9.2-m long and 4.9-m diameter stainless steel chamber. It is evacuated to rough vacuum with one 3800 CFM blower and one 495 CFM rotary-vane pump. Ten-liquid nitrogen cooled shrouded CVI TM-1200i re-entrant cryopumps with a combined pumping speed of 620,000 l/s on argon bring the chamber to a base pressure of 6×10^{-9} torr (measured on N_2). A Stirling Cryogenics SPC-8 RL special closed-looped nitrogen liquefaction system supplies liquid nitrogen to the cryopump shrouds. Two high-vacuum ionization gauges, a Varian model 571 and a Bayard-Alpert model UHV-24, are mounted on opposing sides of the chamber.

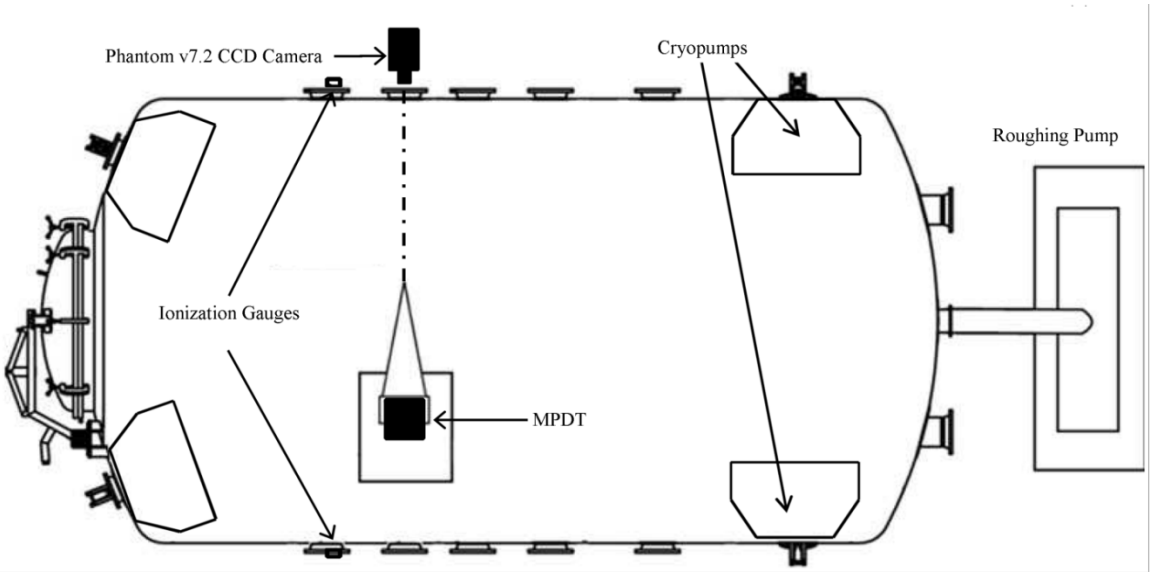

Figure 1. Overhead view of the facility layout (not to scale).

B. MPD Thruster

The thruster features a design similar to the MW-class thruster developed and tested at NASA's Glenn Research Center[2]. The thruster is a self-field design configuration, featuring a ¾-in thoriated tungsten center cathode, 2.5-in wide discharge channel and a 3-in thick stainless steel anode. It is designed to handle power levels above 1 MW in pulsed firing configurations. A frontal view of the thruster assembly is shown in **Figure 2** details a front view assembly of the thruster. Wrapped around the nozzle of the thruster are magnetic nozzle coils. These coils were not used in the testing described in this paper, with the coils instead held at thruster body ground potential during operation.

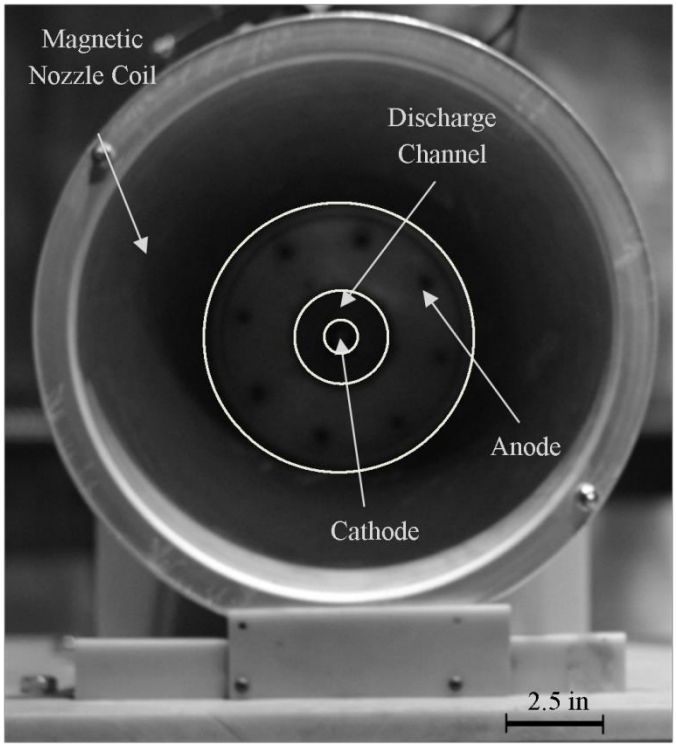

Figure 2. Front View of Thruster Assembly.

C. The Pulse Forming Network

A schematic of the pulse forming network (PFN) is shown in Figure 3. The PFN consists of seven 360-μF, 10-kV metalized-film capacitors with seven wound inductors connected in a Rayleigh line configuration. The total capacitance of the PFN is 2.52 mF with a maximum stored energy of 126 kJ. Because capacitors of equal size are used the impedance of the PFN is high compared to other Guillemin-type networks that can have impedances on the order of the arc resistance ~10 mΩ. The inductors are composed of 2 AWG wire wrapped around 24-in diameter PVC piping, with the winding held in place by Lexan bracketing. The PFN features a custom built 200-mΩ resistive ballast load and an emergency energy dump pathway. A hammer-type tungsten rod switching mechanism controls the PFN pulsing system. PSpice simulations show that under the conditions listed above the PFN can deliver a 10-kA pulse lasting for longer than 3.5 ms. Power is supplied to the MPDT through four 10-kV feed throughs mounted on the flange located closest to the thruster.

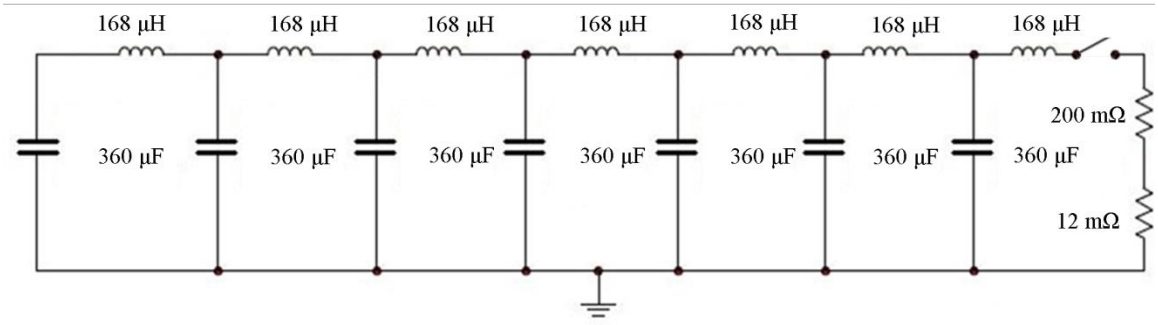

Figure 3. Rayleigh Line Type of PFN. Electrical schematic of the PFN with the 200 mΩ resistive ballast load and 12 mΩ thruster impedance shown on the right-hand side.

D. Pulsed Gas Feed System

The thruster was designed to operate at mass flow rates greater than 0.3 g/s. A pulsed gas feed system like that used in Lapointe and Mikellides[2] was employed to maintain high vacuum levels in VTF-2 during testing at such high mass flow rates. The system features a 117 ft^3 (air), 3000 psi scuba tank as a propellant plenum and an Omega SV251 3-way solenoid valve. A 0.0625-in stainless steel tube serves as a choke in the system. The plenum is connected to a bottle of 99.9995% purity argon and maintained at a constant pressure during thruster operation. Adjustment of the plenum pressure allows for control of the mass flow rate during a pulse. Using the calibration method outlined in Lapointe et al.[2], a mass flow rate uncertainty of less than ±5% is expected. For a gas pulse duration of 1 sec, the background pressure during operation is 7.8 x 10^{-6} - 1.5 x 10^{-5} torr, corrected for argon using the following equation:

$$P_{ar} = P_b + \frac{P_s - P_b}{C} \tag{2}$$

where P_s, P_b, C, and P_{Ar} are the measured pressure, base pressure, the correction factor of 1.29 for argon and the argon-corrected pressure, respectively. Propellant is supplied through a flange that is located at sufficient distance away from the power feed throughs to mitigate any possibility of an electrical arc at the feed through owing to a localized pressure increase.

E. Data Acquisition and Imaging

Based on previous MPDT data, plasma fluctuations during onset are expected to be in the mid-kHz to low MHz range [5]. A Tektronix DPO4045 oscilloscope and a Pearson model 1330 current transformer were used to sample the discharge current profile, which has a maximum measureable peak current of 100 kA and a useable rise time of 0.25 μs. The bandwidth of the oscilloscope is 500 MHz and the maximum sampling rate is 2.5 GS/s. A Tektronix DPO7354C oscilloscope was used to sample the voltage measurements at the anode and cathode obtained with two Tektronik P6015A 1000:1 1 MHz bandwidth high-voltage probes. The voltage across the thruster is found by calculating the difference between the two voltage signals. The bandwidth of the DPO7354C oscilloscope is 3.5 GHz, and it acquires 12-bit data at a sampling rate of up to 100 MS/s. Based on simulated discharges of the PFN and experimental results from[2, 5, 6, 8], the data acquisition system would be sufficient to resolve features in the low MHz frequency range and would be more than sufficient to capture the discharge voltage and current profiles during thruster operation.

A Phantom v7.2 high-speed camera was used to image the discharge. The image size was set to 256 x 256 pixels, yielding a maximum frame rate of 26143 fps. The exposure time for data presented in this paper was 10 μs. The camera was aligned axially with the MPDT, with a 12-in Lexan viewport providing optical access to the thruster during testing (see Figure 1). A 488-nm line filter with a 10-nm bandwidth, corresponding to an argon ion line, was used to capture light emission from the thruster. Additional imaging was performed using a 0.9 neutral density filter (without additional line filtering) to view the overall light emission. Data acquisition for both the oscilloscope and high-speed camera was triggered on the initial current rise as measured by the current transformer. While the voltage fluctuations typical of the onset condition are a higher frequency than what can be imaged at the given frame rate, the large-scale plasma fluctuations are expected to have much lower frequencies [5] [7] and be resolvable by the high-speed camera.

IV. Results

Quasi-steady-state operation of the thruster at discharge currents below onset verified nominal thruster and PFN behavior. Based upon the criteria for achieving onset as given in Eq. (1), the thruster discharge current was increased and the mass flow rate was decreased to achieve onset. To ensure operation above onset, $I^2/\dot{m}$ was greater than 2.77 x 10^{11} A^2-s/kg during testing. Data in Figure 4 (top frame) shows an example waveform where the onset of high frequency voltage oscillations begins shortly after the initiation of the discharge. In all testing, onset was observed for discharge current levels greater than 8 kA. A Fourier transform of these voltage data reveal frequency component peaks at approximately 13 kHz and 82 kHz with the former frequency peak showing an amplitude 5 times greater than the latter. It should be noted that the 82 kHz peak is not sharp in the frequency domain and is broadened over a frequency spectra of approximately 74 kHz-86 kHz. During operation the current (Figure 4 bottom frame) is relatively constant for several ms as desired.

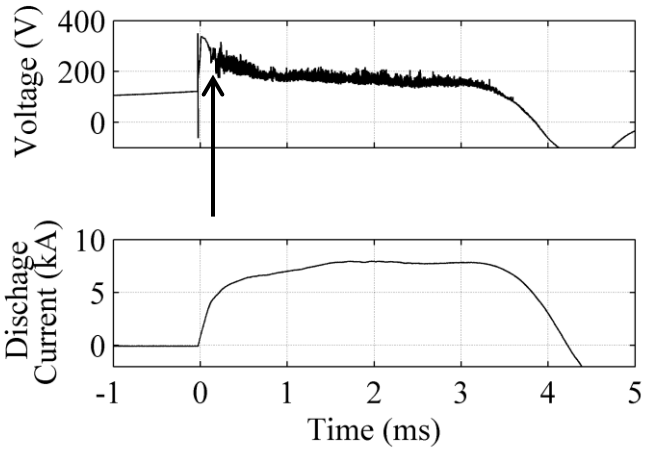

Figure 4. Voltage Traces of MPDT Running in Onset. Voltage (top) and current (bottom) waveforms for a mass flow rate of 0.36 mg/s. The arrow indicates approximate start of onset.

A. Nominal Thruster Operation and Observed Plasma Phenomena

Thruster images acquired through a 488 nm line filter and current waveforms for operation at roughly 10 kA are shown in Figure 5 for a flow rate of 0.36 mg/s. In an effort to push the thruster further into onset, the mass flow rate for the pulse in Figure 6 was reduced by 90% to 0.04 mg/s. In both cases the data exhibit similar start-up characteristics and initial steady-state behavior. Within 0.2 ms of discharge initiation asymmetric plasma formation is observed in both cases. In the second frame of both figures, the steady-state plasma structure is mostly formed. Throughout the pulse, asymmetries are observed that are consistent with the shape of a plasma column. In addition a bright concentrated secondary plasma structure can be seen as a steady-state plasma characteristic on the surface of the center cathode. .

The thruster typically experiences current ring-back on the order of -3 kA. Figure 6 shows an operating pulse where the coupling of the PFN to the transmission line failed, leading to premature discharge extinction without the typical ring back observed in other trials. The sudden loss of current leads to a loss in plasma confinement within the thruster. In Figure 6, the plasma extinguishes 1.5 ms after frame D.

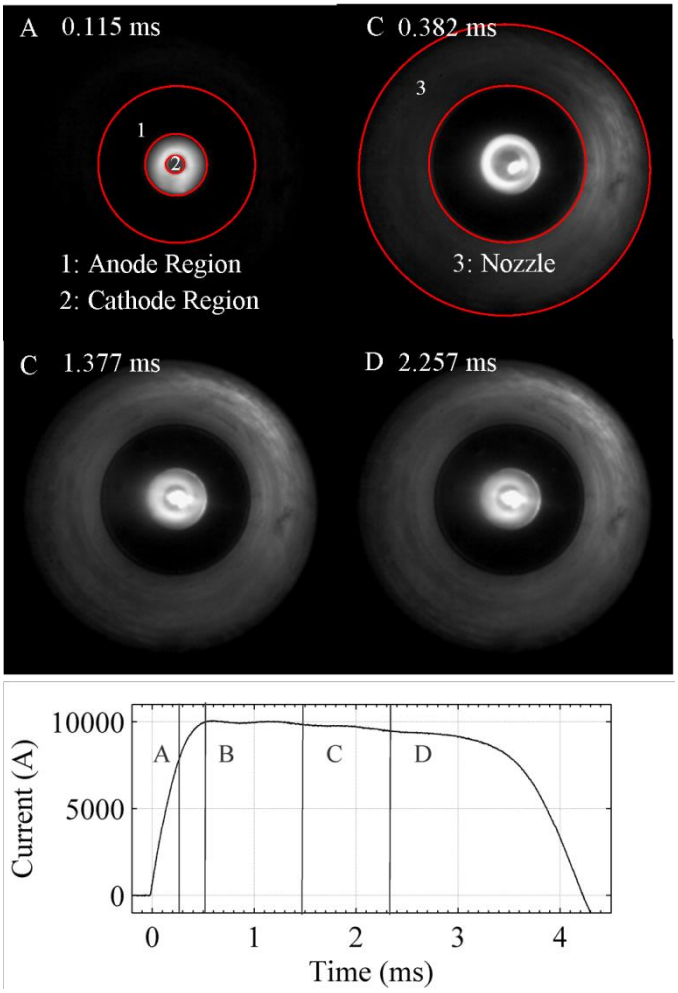

Figure 5. MPDT time-resolved images. Obtained with a 488 nm line filter (top) and discharge current waveform (bottom) for a flow rate of 0.36 mg/s . The time corresponding to each image is given on the current waveform.

B. Cathode Ablation and Particulate Ejection

In addition to imaging the discharge, we directly observed the ablation of cathode material as it was ejected from the thruster. Erosion of cathode material is typical in MPDTs [16].The cathode, typically comprised of a refractory metal, experiences significant thermal stress owing to the high discharge currents, causing some of the surface material to be ablated and ejected during the pulse. Low-speed, time-integrated 166.7 ms exposure time images of the thruster are shown in Figure 7. In Figure 7a the entire thruster pulse is captured in the image, while in Figure 7b the camera imaging was time-delayed so that only the portion of the discharge occurring after the current rings through zero is observed. These images were captured with a Canon T3i DSLR camera. Both images show substantial ablation products in the thruster exhaust, which appear as straight-line streaks.

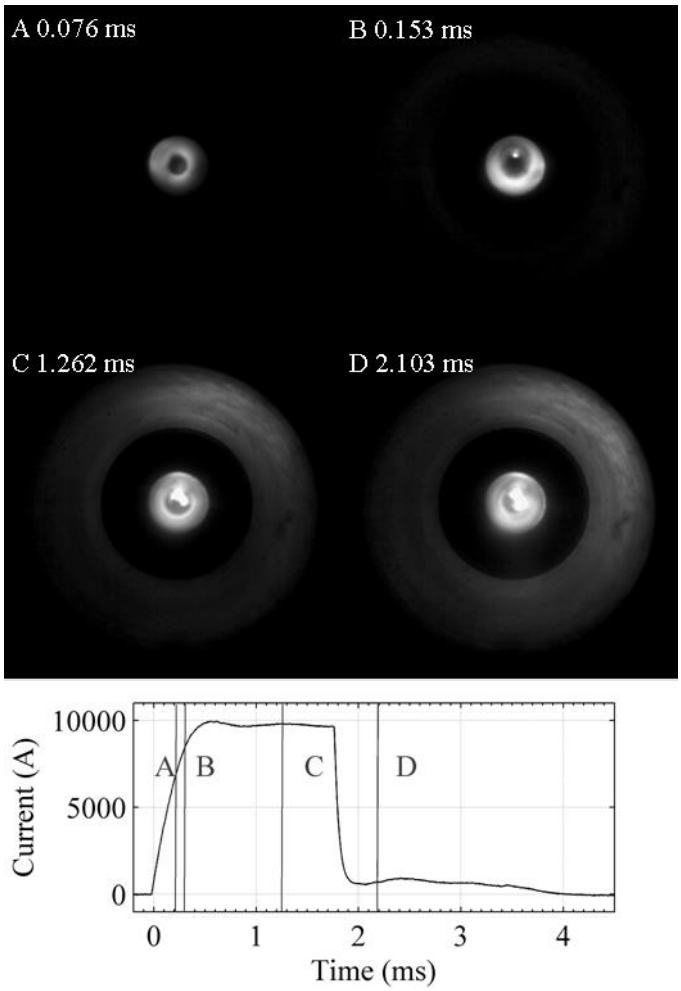

Figure 6. MPDT time-resolved images. Obtained with a 488 nm line filter (top) and discharge current waveform (bottom) for a flow rate of 0.04 mg/s . The time corresponding to each image is given on the current waveform.

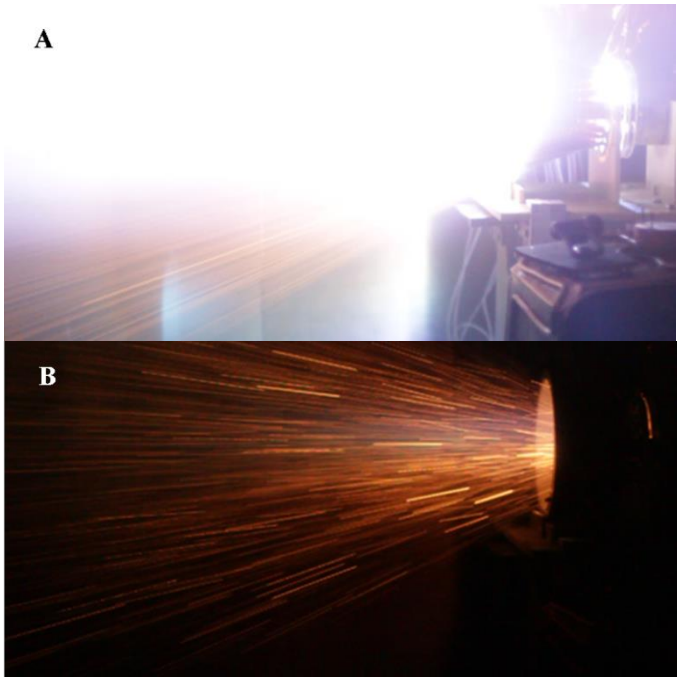

Figure 7. Time-integrated images of MPDT. For an exposure time of 166.7 ms showing (a) an exposure containing the quasi-steady-state thruster operation and (b) an exposure containing only the current ring-back portion of the discharge.

High-speed imaging was performed using a 0.9 neutral density filter at a reduced exposure time to 7 μs. Time-resolved images of the discharge during the current reversal phase are presented in Figure 8, above the current waveform. In Figure 8, the creation and ejection of a single ablated particle is tracked, with a circle in each frame highlighting the initial appearance and subsequent trajectory of the particle as it travels away from the cathode surface. High-speed imaging of thruster operation showed substantial numbers of these cathode particles being ejected from the thruster throughout the discharge.

Post-test inspection of the thruster revealed that both the cathode and anode surfaces were marred by erosion. For comparison, pre- and post-test images of the thruster are presented in **Figure 9**. We observe that before testing that the cathode had a sharp point and the anode surface was free of defects. After over 40 pulses the cathode tip has been visibly blunted and the anode surface is marred in a manner consistent with operation in the onset regime. While both the cathode and anode experience erosion, the high-speed imaging in Figure 8 shows that the cathode is the source of most of the ablation products observed in the time-integrated photographs of Figure 7.

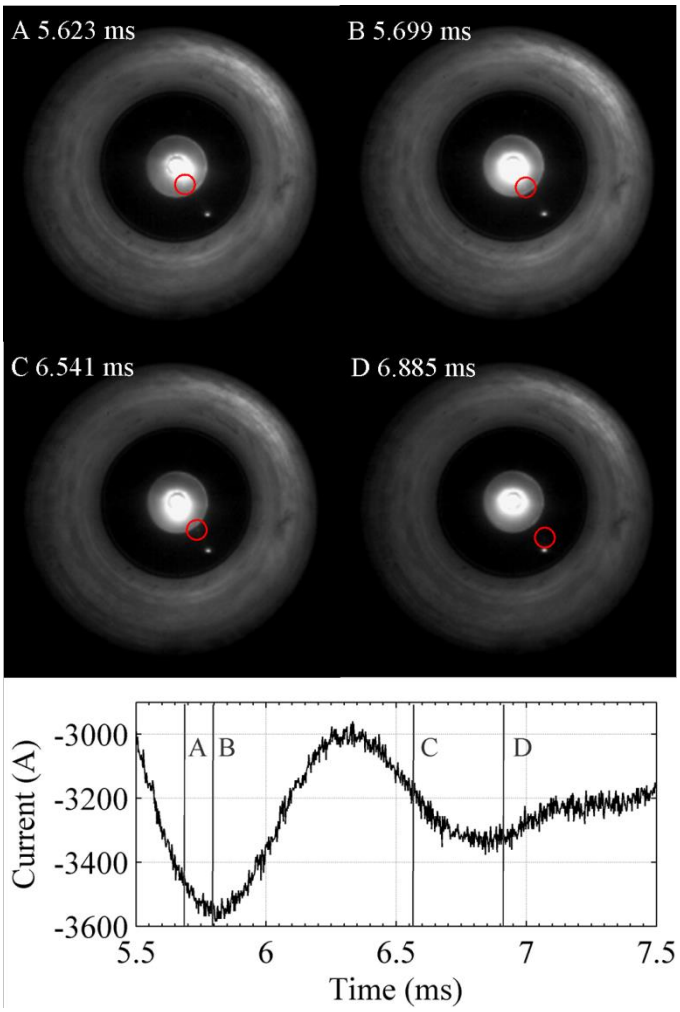

Figure 8. MPDT Time-Resolved Images. Obtained with a 0.9 neutral density filter (top) and discharge current waveform (bottom) during current reversal. The time corresponding to each image is given on the current waveform and the circle from frame to frame tracks an individual ejected particle's trajectory.

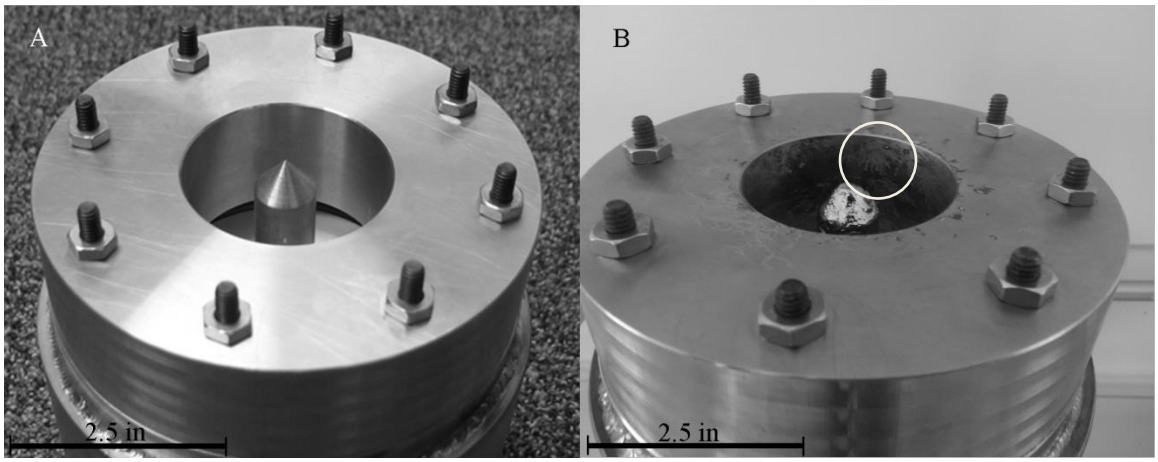

Figure 9. (A) Before and (B) after images of the thruster after several pulses showing the effects of erosion on the cathode and anode. The circle in (B) highlights an area of anode erosion.

V. Discussion

The imaging presented in the previous section shows visual evidence of discharge asymmetries that could be the manifestation of lower-order mode kink instabilities. We proceed by investigating whether the discharge plasma column exhibits the key topographic features expected in the kink mode and determine if the operating conditions in the thruster are that have been linked to this type of in a mode that can excite this instability. A more detailed analysis of the imaging is now presented to further investigate these lines of reasoning.

A. Helical Structure of the Discharge

To quantitatively analyze the discharge plasma, the imaging values for each pixel were first converted from unit-less unassigned 8-bit numbers to values that have physical meaning. The sensor properties of the Phantom v7.2 camera are shown in Table I. This enables the calculation of the power flux to the individual pixels of the camera using the raw image data. The sensor conversion is linear throughout the electron full-well range of the charged couple device (CCD). The 488-nm notch filter ensures that the power flux incident on the CCD array is directly correlated to emission from argon ions. Note that the light collected by the camera will be lower in intensity than the light initially emitted by the thruster, owing to absorption by the optical window and other optics and refraction of light by the air between the vacuum chamber window and the camera lens. The calculated visual power fluxes are show in Figure 10 for the same images that were presented in Figure 5. In these images the regions of intense power flux correlate to regions of plasma concentration.

Table I Phantom v7.2 Sensor Properties

Spectral Response @ 488 nm	Full Well Capacity, electrons	Pixel Size, μm
28%	22×10^3	6

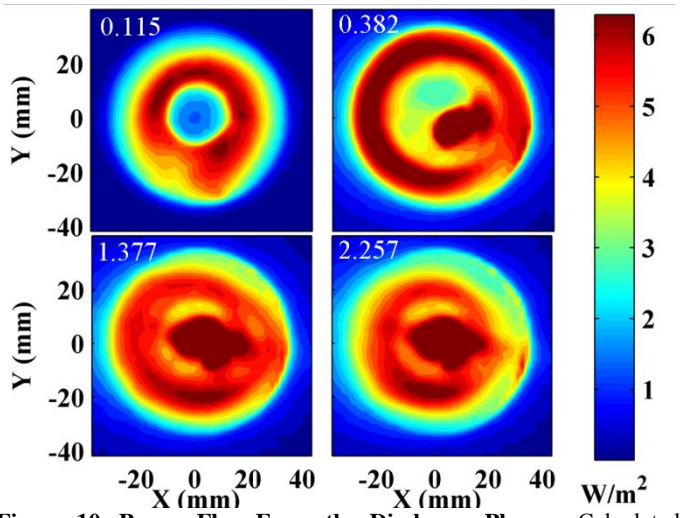

Figure 10. Power Flux From the Discharge Plasma. Calculated using the collected visual light incident on the CCD presented in Figure 5.

In previous open-ended co-axial accelerator experiments, the lower-order kink mode instabilities manifest through a helical-shaped plasma column[5-7]. The time-resolved asymmetrical topology of the discharge plasma in Figure 10 is often representative of excitation of helical-shaped lower-order kink modes. To connect what was imaged during the thruster operation to the kink mode instability, we must show that the images of the discharge plasma could have a helical shape. What is immediately clear from the processed imaging in Figure 10 is that the concentration of plasma is asymmetric. The measured power flux in these images are line-integrated axially, so to say that the images are of a plasma column that is helical requires consideration on how a three dimensional helical geometry would appear when represented as a two dimensional image. Paganucci[7] concluded that the helical plasma column should only contain one pitch of the m=1, n=1 kink mode. In other words, the discharge plasma column only wraps around the cathode once. This suggests that the measured power flux should be not only asymmetric due to a non-uniform axial distribution of the plasma, but that the power flux intensity should also exhibit an azimuthal growth from one clock position around the discharge channel back to the same clock position.
The time resolved behavior of the observed discharge plasma exhibit characteristics expected of the kink mode instabilities. At time 0.115 ms, the formation of the plasma column is centrally located around the cathode of the thruster. This plasma formation moves radially outwards towards the anode of the MPDT as seen at time 0.383 ms. After contact is made with the anode wall, the plasma column "locks in" and holds a quasi-steady-state position throughout the remainder of the discharge pulse (shown for 1.377 ms and 2.257 ms). Also in the frames at 1.377 ms and 2.257 ms, we observe that the plasma exhibits the described azimuthal non-uniformity at the anode wall starting near the 2 o'clock position and growing counter clockwise until the 5 or 6 o'clock position. These behaviors are similar to those of Paganucci et al.[7], suggesting that we are observing the excitation of a lower order kink mode. The lack of azimuthal detail in the transient images is attributed to an expected transient rotational frequency greater than 50 kHz, which is much faster than the frame rate of the camera [7]. From frame-by-frame analysis of the initial current rise, the measured radial propagation velocity of the discharge plasma from the cathode surface to the anode wall during discharge initiation is on the average 3300 (+80,-60) m/s. This measurement is made through observations of the propagating edge of the discharge plasma. The discharge plasma propagation behavior as seen in Figure 10 repeats itself in other test firings above 9 kA of discharge current. Because the clocking of the discharge plasma asymmetries varies between thruster firings, we conclude that the plasma column asymmetries are not heavily influenced due to physical defects in the anode surface; for example, surface scratches and geometric asymmetries. At discharge currents below 8 kA, a more uniform, axisymmetric discharge plasma column is observed; although, the plasma during discharge initiation still executes the same coherent radial propagation as seen in the higher current level cases. These current levels may represent a transitional stability regime for the discharge plasma. However this is only a speculative hypothesis at this time and the data and analysis to confirm this are beyond the scope of the present work.

B. Kruskal-Shafranov limit

A theoretical result used to predict the presence of MHD plasma instabilities is the Kruskal-Shafranov limit. Classically, a linear perturbation of the MHD governing equations for an axisymmetric plasma column leads to the derivation of the following criteria for plasma column stability,

$$q(r) = \frac{2\pi B_z r}{B_\theta(r) L} > 1, if\ stable \tag{3}$$

where $B_z, B_\theta, r,$ and L are the axial magnetic field, the azimuthal magnetic field, the distance away from the center of the plasma column and the length of the plasma column. When discussing overall plasma stability, we must confine ourselves to the boundary region of the plasma column, permitting us to recast Equation 3 as

$$q(a) \equiv \frac{2\pi a^2 B_z}{\mu_0 J_o L} > 1\ , if\ stable \tag{4}$$

where $B_z, \mu_0, J_o,$ a, and L are the axial magnetic field, permeability of free space, total plasma current, plasma column diameter and plasma column length, respectively[17]. This criterion gives rise to what the fusion community calls q or the safety factor. Specifically, this limit applies to the edge of the plasma column where the instability will first manifest itself. When q is below 1, the internal pressure forces exceed the magnetic pressure forces, and the m=1 n=1, first kink mode becomes unstable. In a self-field configuration this classical stability criteria may not seem directly applicable. The ideal MPDT treatment assumes that there is only an azimuthal magnetic field generated by the current flowing through the cathode. In reality, there is non-uniform, non-axisymmetric radial cross-channel current mobility from the cathode to the anode, as shown in plasma contour simulations of various MPDTs[18, 19]. This cross-channel current can give rise to axial magnetic field components; thus the magnetic field topology has components in both the azimuthal and downstream direction. Thus, we can expect the MPDT magnetic field in regions of high current density has strong azimuthal components and weak axial components. From Equation 3, we see that this ratio (B_z/B_θ) is important in determining plasma column stability and can conclude that this ratio is much less than unity. In the geometric component of the safety factor (r/L) is really a dependence on the ratio between the plasma column radius and length. From Paganucci et al[7], this aspect ratio tends to be small and is directly related to the pitch of the helical kink. The on-axis thruster imaging from Figure 10 cannot yield an exact measurement of the pitch or length; however the plasma column width can be estimated at approximately 1 cm. Given that the diameter of the MPDT is 6.35 cm and the discharge channel depth is 7.62 cm, the geometric ratio of the plasma column is on the order of 0.01 or lower. Direct measurements of the magnetic field within the thruster would yield further evidence of this instability, but the diagnostic capability needed to perform this measurement was not included in the presented experimental campaign. However, to first-order we have shown that both the ratio of the magnetic field components and the geometric aspect ratio from comprising Equation (**3** are expected to be small. Thus, the safety factor must be near or below 1, implying that the discharge plasma column in the thruster is below the Kruskal-Shravnov limit and therefore prone to instability.

VI. Conclusion

We have presented measurements on a self-field quasi-steady-state MPDT that was operated at currents above 8 kA where onset behavior is observed. The parameters within the thruster are such that it appears to be operating in the unstable plasma regime described by the Kruskal-Shravnov stability limit and previous thruster experiments have exhibited excitation of kink mode instabilities during operation in the onset regime. Fast imaging of the discharge shows a plasma that contains asymmetrical features consistent with a helical-shaped plasma column that is characteristic of a lower-order kink mode instability. We conclude that the discharge plasma topology imaged during thruster operation is a manifestation of the lower order kink mode instabilities. The data show that the onset phenomena and the appearance of the kink mode instability could be closely correlated, presenting a path for future investigations.

Acknowledgments

J.A. Walker would like to thank the National Science Foundation Graduate Research Fellowship Program for funding that enabled this research to be accomplished. I am grateful for the efforts of Nicole Tyman and Joshua Mann for their assistance in the installation and operation of the MPDT support facilities.

K.A. Polzin and A.C. Kimberlin acknowledge NASA Marshall Space Flight Center management support from Jim Martin, J. Boise Pearson, Mary Beth Koelbl, Thomas Williams, and Paul Mcconnaughey. We are grateful to Craig Garrison for the loan of the Phantom v7.2 camera that made this work possible.

References

1. Goebel, D. M., and Katz, I. *Fundamentals of Electric Propulsion: Ion and Hall Thrusters*: John Wiley & Sons, 2008.
2. LaPointe, M., and Mikellides, P. G. "High power MPD thruster development at the NASA Glenn Research Center," *37th Joint Propulsion Conference*. American Institute of Aeronautics and Astronautics, Salt Lake City, Utah, 2001.
3. Wagner, H. P., Kaeppeler, H. J., and Auweter-Kurtz, M. "Instabilities in MPD thruster flows: 2. Investigation of drift and gradient driven instabilities using multi-fluid plasma models," *Journal of Physics D: Applied Physics* Vol. 31, No. 5, 1998, pp. 529-541.
doi: 10.1088/0022-3727/31/5/010
4. Wagner, H. P., Kaeppeler, H. J., and Auweter-Kurtz, M. "Instabilities in MPD thruster flows: 1. Space charge instabilities in unbounded and inhomogeneous plasmas," *Journal of Physics D: Applied Physics* Vol. 31, No. 5, 1998, pp. 519-528.
doi: 10.1088/0022-3727/31/5/009
5. Paganucci, F., Zuin, M., Agostini, M., Andrenucci, M., Antoni, V., Bagatin, M., Bonomo, F., Cavazzana, R., Franz, P., Marrelli, L., Martin, P., Martines, E., Rossetti, P., Serianni, G., Scarin, P., Signori, M., and Spizzo, G. "MHD instabilities in magneto-plasma-dynamic thrusters," *Plasma Physics and Controlled Fusion* Vol. 50, No. 12, 2008, p. 124010.
doi: 10.1088/0741-3335/50/12/124010
6. Zuin, M., Cavazzana, R., Martines, E., Rossetti, P., Signori, M., Andrenucci, M., and Paganucci, M. "Investigation of MHD Instabilities in an Applied Field MPD Thruster by Means of Measurement of Magnetic Field Fluctuations," *International Electric Propulsion Conference*. Ann Arbor, MI, 2009.
7. Paganucci, F., Andrenucci, M., Agostini, M., Antoni, V., Zuin, M., Spizzo, G., Martin, P., Bonomo, F., Franz, P., Bagatin, M., Cavazzana, R., Marerelli, L., Martines, E., Rossetti, R., Signori, M., Serianni, G., and Scarin, P. "Further Experimental Evidences of the Development of Kink Instabilities in MPD Thrusters," *41st AIAA/ASME/SAE/ASEE Joint Propulsion Conference & Exhibit*. American Institute of Aeronautics and Astronautics, 2005.
8. LaPointe, M. R. "Numerical Simulation of Cylindrical, Self-Field MPD Thrusters with Multiple Propellants," *International Electric Propulsion Conference*. Seattle, Washington, 1993.
9. Wagner, H. P., Kaeppeler, H. J. and Auweter-Kurtz, M. "Instabilities in MPD Thruster Flows: 2. Investigation of Drift and Gradient Driven Instabilities using Multi-Fluid Plasma Models," *Journal of Physics D: Applied Physics* Vol. 31, No. 1998, 1997, pp. 529-541.
10. Andrenucci, M., and Paganucci, F. "Fundametal Scaling Laws for Electric Propulsion Concepts," *Joint Propulsion Conference*. 2004.
11. Park, H. K. "A new asymmetric Abel-inversion method for plasma interferometry in tokamaks," *Plasma Physics and Controlled Fusion* Vol. 31, No. 13, 1989, pp. 2035-2046.
doi: 10.1088/0741-3335/31/13/007
12. Schrade, H., Auweter-Kurtz, M., and Kurtz, H. L. "Stability problems in magneto plasmadynamik Arc thrusters," *AIAA 18th Fluid Dynamics and Plasmadynamics and Lasers Conference*. American Institute of Aeronautics and Astronautics, Cincinatti, Ohio, 1985.
13. Zuin, M., Cavazzana, R., Martines, E., Serianni, G., Antoni, V., Bagatin, M., Andrenucci, M., Paganucci, F., and Rossetti, P. "Critical regimes and magnetohydrodynamic instabilities in a magneto-plasma-dynamic thruster," *Physics of Plasmas* Vol. 11, No. 10, 2004, p. 4761.
doi: 10.1063/1.1786593
14. Kagaya, Y., Tahara, H., and Yoshikawa, T. "Effect of Applied Magnetic Nozlle in a Quasi-Steady MPD Thruster," *International Electric Propulsion Conference*. Toulouse, France, 2003.
15. Hsu, S., and Bellan, P. "Experimental Identification of the Kink Instability as a Poloidal Flux Amplification Mechanism for Coaxial Gun Spheromak Formation," *Physical Review Letters* Vol. 90, No. 21, 2003.
doi: 10.1103/PhysRevLett.90.215002
16. Schrade, H. O., Auweter-Kurtz, M., and Kurtz, H. L. "Cathode erosion studies on MPD thrusters," *AIAA Journal* Vol. 25, No. 8, 1987, pp. 1105-1112.
doi: 10.2514/3.9750

17. Oz, E., Myers, C. E., Yamada, M., Ji, H., Kulsrud, R. M., and Xie, J. "Experimental verification of the Kruskal-Shafranov stability limit in line-tied partial-toroidal plasmas," *Physics of Plasmas* Vol. 18, No. 10, 2011, p. 102107. doi: 10.1063/1.3647567